Desalination and Water Treatment
www.deswater.com

1944-3994/1944-3986 © 2012 Desalination Publications. All rights reserved
doi: 10/5004/dwt.2012.1917

37 (2012) 38–45
January

Taylor & Francis
Taylor & Francis Group

Direct impact and delayed post-discharge chemical reactions of Fe^{II} complexes induced by non-thermal plasma

Samuel Laminsi[a], Elie Acayanka[a], Serge Nzali[a], Peter Teke Ndifon[a], Jean-Louis Brisset[b,*]

[a] *Inorganic Chemistry Department, University of Yaounde-I, P.O. Box 812, Yaounde, Cameroon*
[b] *Laboratoire d'Electrochimie (L.E.I.C.A.), UFR des Sciences de l'Université de Rouen, 76821 Mont-St. Aignan, France*
Email: brissjl@club-internet.fr

Received 12 March 2010; Accepted 30 June 2011

ABSTRACT

Dilute solutions of organometallic complexes, i.e., Ferrocene and *tris*(1,10-phenanthroline)Fe^{II} or ferroïn, readily oxidize when exposed to the gaseous species generated in a gliding electric discharge in humid air. Ferrocene (or *bis*-cyclopentadienyl Fe^{II}) turns to blue ferricinium ion while ferroïn solutions fade. Ferroïn is gradually oxidized to ferriïn which agrees with the higher sensitivity of the central metal to the action of plasma than the organic ligand engaged in the complex. The oxidation hardly obeys a pseudo 1st order kinetics law ($k_1^* = 4 \times 10^{-2}$ min^{-1}). Additionally the oxidation reaction keeps on developing in post-discharge conditions according to a pseudo 1st order reaction ($k_1 = 5 \times 10^{-3}$ min^{-1}). This feature tends to generalize the occurrence of temporal post-discharge reactions which are of major interest for industrial applications.

Keywords: Gliding discharge; Non-thermal plasma; *tris*(1,10-phenanthroline)$_3Fe^{II}$; Ferrocene; Post-discharge; Humid air; Oxidation

---

1. Introduction

Using electric discharges as convenient sources of non-thermal plasma at atmospheric pressure becomes familiar to people concerned with pollutant abatement and bacterial inactivation because of the particular chemical properties of the gaseous species which compose the plasma. The main chemical properties induced in a liquid solution exposed to the discharge depend on working conditions, e.g., the nature of the ambient gas or the presence of catalysts. However one kind of reaction is usually observed at the liquid surface of the treated solution, i.e., at the plasma-liquid interface. For example discharges in humid air produce strong reacting oxidizers over the target.

We are concerned in this paper with a particular type of discharge – the gliding discharge or "glidarc"– which burns at atmospheric pressure and belongs to the family of the non-thermal plasmas because it is actually a quenched plasma. When two diverging conductors, i.e., the electrodes, are connected with an electrical energy source such as a high voltage transformer, an arc (i.e., a thermal plasma) forms at the narrowest electrode gap. The arc feet are pushed along the electrodes by a gas flow directed along the axis of the reactor: the arc length increases and its temperature decreases until arc breaking takes place at the electrode tips and the thermal plasma turns to a quenched non-thermal plasma in the plasma plume. The arc breaking occurs when the gliding arc is short-circuited by a new one which resumes the cycle. The gliding arc was proposed several decades ago by Czernichowski and co-workers with Orleans University (Gremi Lab) for gas treatments and later developed with Rouen University (LEICA) for liquid treatments [1,2].

---

*Corresponding author.

1.1. An overview of the chemical properties of a gliding discharge in ambient humid air

Discharges in humid air are known to induce acid and oxidizing effects in an aqueous target solution. A part of the thermal energy carried on by the arc is transferred to the surrounding "parent species" of the ambient gas and thus favours the breaking of H—OH and O=O bonds. This feature requires less energy than N≡N bond breaking and allows rising gaseous moieties from their fundamental energy level to some excited state.

Thus, the $^\circ NO$ and $^\circ OH$ radicals mainly formed in the arc by electron impact were identified and quantified by emission spectroscopy are the determining agents for the chemical reactions observed in the target solution [3].

$$H_2O + e- \rightarrow H^\circ + {}^\circ OH + e- \tag{1}$$

$$H_2O + e- \rightarrow H^+ + {}^\circ OH + 2\ e- \tag{2}$$

$$O_2 + e- \rightarrow 2O^\circ + e- \tag{3}$$

$$N_2 + O^\circ \rightarrow NO^\circ + N^\circ \tag{4}$$

Fig. 1. illustrates the distribution of the main active species in the gas phase and accounts for reactions occurring between gaseous species. The parent species refer to the ambient gas components, O_2, N_2, H_2O and give rise to the primary species by interacting with the discharge.

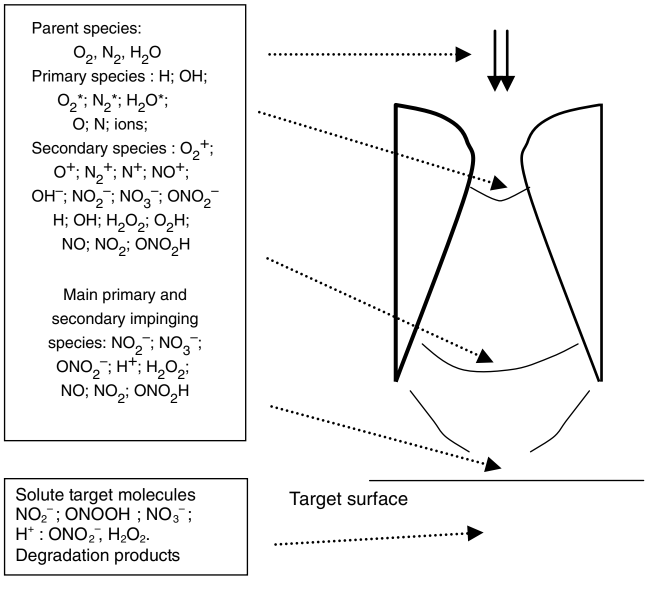

Fig. 1. Scheme of the distribution of parent, primary and secondary species in a gliding discharge.

The primary species react both with themselves and the parent species to form secondary species according to the following main reactions in the gas phase:

$$N^\circ + O^\circ \rightarrow {}^\circ NO \tag{5}$$

$$O_2 + O^\circ + M \rightarrow O_3 + M \tag{6}$$

$$O_3 + {}^\circ OH \rightarrow O_2 + {}^\circ O_2H \tag{7}$$

$$O_3 + {}^\circ NO \rightarrow {}^\circ NO_2 + O_2 \tag{8}$$

$${}^\circ NO_2 + {}^\circ OH \rightarrow ONO_2H \tag{9}$$

The formation of ozone is known not to be favoured by the presence of water molecules and O_3 readily disappears by reacting with $^\circ OH$ and $^\circ NO$ Eqs. (7, 8). $^\circ O_2H$ remains as traces due to the the reactions with $^\circ NO$ and $^\circ O_2H$ Eqs. (10,11) according to slightly different mechanisms:

$${}^\circ NO + {}^\circ O_2H = {}^\circ NO_2 + {}^\circ OH \tag{10}$$

$${}^\circ O_2H + {}^\circ O_2H \rightarrow H_2O_2 + O_2 \tag{11}$$

The reactive radicals $^\circ OH$ and $^\circ NO$ react both with themselves and the parent species as mentioned, and are thus present in the quenched plasma plume, so that the impinging active species in contact with the liquid surface are mainly H_2O_2 and Nitrogen oxides Eqs. (12–14).

$$2{}^\circ OH \rightarrow H_2O_2 \tag{12}$$

$${}^\circ NO + {}^\circ O \rightarrow {}^\circ NO_2 \tag{13}$$

$${}^\circ NO_2 + {}^\circ OH \rightarrow ONOOH \tag{14}$$

$$ONOOH \rightarrow NO_3^- + H^+ \tag{15}$$

$^\circ NO$ is responsible for the formation of nitrous acid (via $^\circ NO_2$) which disproportionates into $^\circ NO$ and NO_3^- in acidic solution but also yields peroxynitrous acid ONOOH Eq. (14), which later isomerizes into nitric acid Eq. (15). This compound is therefore involved as a source of the acid and oxidizing properties of the plasma [2]. The standard oxidation potentials of the relevant couples are gathered in Table 1. The targeted solution then enriches with protons, nitrate ions and other reaction products due to overall strong acid and oxidizing effects of the discharge which are directly related with temporal post-discharge reactions [2].

Table 1
Pertinent oxidation reduction systems and relevant standard potentials

$Ox + qH^+ + ne^-$	↔	Red	$E°(Ox/Red)$, V/SHE
$°OH + H^+ + e^-$	↔	H_2O	2.85
$ONOO^- + 2H^+ + e^-$	↔	$°NO_2 + H_2O$	2.44
$O_3 + 2H^+ + 2e^-$	↔	$O_2 + H_2O$	2.07
$ONOOH + H^+ + e^-$	↔	$°NO_2 + H_2O$	2.05
$H_2O_2 + 2H^+ + 2^{e-}$	↔	$2H_2O$	1.68

The number of active species formed in the discharge makes the plasma gas a complex medium and a source of numerous reactions which apply to a variety of situations. This explains why plasma gases find so many industrial applications, such as gas cleaning, pollution control, fuel conversion, hydrogen production and surface treatments [4–9]. However serious difficulties with the plasma technique lie in the lack of specific properties, as a direct consequence of the numerous reactions involved in the discharge. Research now focuses on modifying the gas composition to favour one type of induced reactions. A matching problem is connected with identifying and quantifying the active species: physical methods such as emission spectrometry or Laser Induced Fluorescence are suitable tools for the purpose because most of the chemical characteristic chemical reactions are not specific. For example iodometry titration of ozone is trustable in case of pure ozone, but fails when other strong oxidizing species are present.

1.2. The twin aims of the study

Selecting a coloured indicator system with a high standard oxidation potential is expected to limit the number of interfering systems [10,11]. This is among our main purposes, so that a given indicator system might be used for titration to account for the overall oxidizing power of the plasma species. Consequently we first selected iron complexes: preliminary tests performed on ferrocene solutions confirmed the oxidizing power of the humid air plasma and showed that the formation of the blue ferricinium ion preceded the degradation of yellow ferrocene. Another coloured complex, i.e., the *tris*(1,10-phenanthroline)Fe^{II} (or ferroïn) complex was selected for its colour change between the reduced and the oxidized forms and for the relevant high oxidation potential of the ferriïn/ferroïn system. Evolution of aqueous solutions of ferroïn was thus followed by means of spectrometry measurements for various direct exposure times t^*(min) to the discharge. Absorbance measurements at the absorption peaks [11] brought information on the kinetic mechanism. Thus, oxidation reduction indicators are required in a similar way as acid-base indicators are employed to mark sharp pH changes in acid-base titrations [10]. A matching aim of the study is using an ideal overall oxidation-reduction indicator to account for both oxidation of the solute immediately after direct exposure to the discharge and after a delay in TPDR conditions.

Additionally, we aimed to check the occurrence of temporal post-discharge reactions (TPDR) on this example [2]. TPDR refer to reactions which develop in plasma treated solutions after the discharge is switched off and in the absence of extra provided energy: they are observed without direct impact of the plasma species at the target solute during the post-discharge. The study of the selected complex under TPDR conditions aims to confirm the general character of this feature.

2. Materials and methods

2.1. Materials

Ferrocene (Fc) or *bis*(cyclopentadienyl) iron(II) was purchased from Acros and sparingly dissolved in deionized water. The oxidized form, ferricinium (Fc^+) is more soluble than Fc, and its structure slightly differs from Fc since the cyclopentadienyl rings present an angle by a few degrees. The system Fc^+/Fc was very popular around the seventies because the solvation of oxidized and reduced forms were assumed to be independent of the solvent: thus the standard potential of the Fc^+/Fc system was considered by several scientists as a reference potential to evalutate the transfer activity coefficient of the proton between water and any organic solvent or solvent mixture.

All basic analytical grade reagents were used without further purification. The *tris*(1,10-phenanthroline) Fe^{II}, referred to as $Fe^{II}L_3$, was prepared from 1,10 phenanthroline (Aldrich) and ferrous sulphate (Riedel de Han) according to standard procedure and recrystallized two times in ethanol.

The organometallic compound is used as an oxidation-reduction indicator, due to its characteristic colour changes with the applied potential [11]. The ligand presents basic properties with a pK_a close to 4.9 [11]. Several metal-ligand complexes are known and the cumulative stability constants log β_i are gathered in Table 2 with spectral characteristics relevant to the maximum 1:3 complexes.

Ferroïn $Fe^{II}L_3$ is the reduced form associated with the oxidized form, ferriïn $Fe^{III}L_3$:

$$Fe^{II}L_3 \leftrightarrow Fe^{III}L_3 + e^-$$

The reversibility of the system is largely accepted and its behaviour is thus governed by the Nernst equation

Table 2
Analytical data relevant to Fe-phenanthroline complexes

	log β_1	log β_2	log β_3	λ_{peak}, nm	ε_{peak}
$Fe^{II}L_n$	5.9	11.1	21.3	510	11100
$Fe^{III}L_n$			14.1	590	600

$$E = E°(Fe^{III}L_3/Fe^{II}L_3) + \left(\frac{RT}{F}\right) \mathrm{Ln}\,\frac{a_{Fe^{III}L_3}}{a_{Fe^{II}L_3}} \qquad (16)$$

where $E°$ = 1.14 V/SHE is the standard oxidation potential of the ferroïn/ferriïn system and a_i refers to the activity of the solute *i*.

2.2. Experimental apparatus used for plasma treatments

The scheme of a gliding discharge set-up [12] is given in Fig. 2. It involves a couple of aluminium electrodes symmetrically disposed on both sides of an atomizing nozzle (Diameter: 1 mm) and connected to an AC 220 V/10 kV-1A high voltage transformer which delivers a mean current intensity 160 mA (600 V) in operating conditions (P # 100 W). The selected feeding gas was water saturated air provided by a compressor and passing through a bubbling flask before entering the reactor. Water-air was sprayed directly into the zone formed between the electrodes through an atomizing nozzle. An arc is formed between the electrodes when a high voltage is applied. The arc is then pushed away by the bi-phase flow from the nozzle and glides along the electrodes until it collapses. The arc length increases on moving and its temperature decreases, so that the arc turns from a thermal plasma to quenched plasma on breaking into a plume. A new arc then forms at the narrowest gap and the cycle resumes as a large plasma plume in contact with the liquid surface allows chemical reactions to develop. The target solution is thus directly exposed to the plasma plume for time *t**(min) [2,6,13].

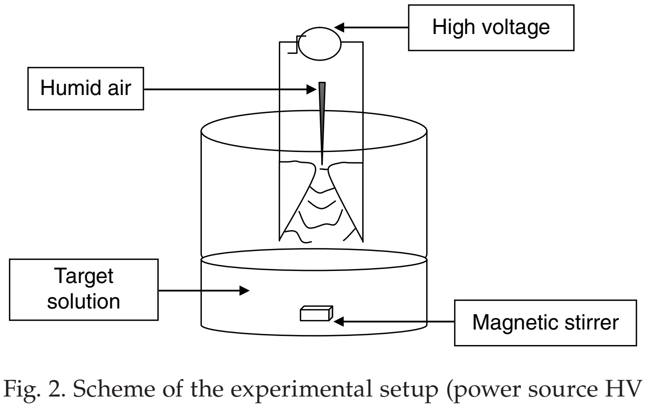

Fig. 2. Scheme of the experimental setup (power source HV transformer 10 kV-1 A; distance from electrode tips to liquid target *d* = 50 mm).

2.3. Treatment and analysis procedures

The treatments were carried out using batch reactor conditions for time *t**. The target solution of 1,10-Phenanthroline complex (450 ml; 50 mg/l) was disposed normally to the axis of the water cooled glass reactor (Fig. 2) at a distance of about 50 mm from the electrodes tips. The solution was magnetically stirred. The gas flow rate of the water saturated gas was optimized at 800 $l \cdot h^{-1}$ before entering the reactor .

Evolution of the composition of the targeted solution was followed by spectrophotometric investigation. The spectra at 25 ± 0.03°C were recorded with a UV-Vis spectrophotometer model Aqualytic SpectroDirect and absorbance measurements were made with the same instrument at the absorption peaks (Table 2). Solutions were exposed to the plasma for different exposure times *t** (i.e., 0, 0.5, 1, 2, 5, 10, 15, 20 and 30 min). After the discharge was switched off, an aliquot of the exposed solution was immediately analyzed; while another one was kept in the dark and at low temperature before being analysed for different post-discharge times (i.e., *t* = 0, 5, 10, 20, 30, 40 and 60 min).

3. Results and discussion

Oxidation of ferrocene into ferricinium demonstrates that electron exchange takes rapidly place before the destruction of the complexes becomes significant.

The base 1,10-phenanthroline readily combines in solution with iron(II) ($[Fe(II)(H_2O)_6]^{2+}$, S = 2, spin) in the molecular ratio 3:1 (i.e., base 1,10-phenanthroline: iron (II) ion), forming the intensely red complex $[Fe(II)(o\text{-phen})_3]^{2+}$ which absorbs at 515 nm. The color intensity is independent of the medium acidity in a large pH range and it is stable for long periods [11].

3.1. Effect of exposure time on the oxidation of ferroïn complex

Fig. 3 reports the spectral changes of the starting complex after being exposed to the discharge for time *t**(min). The spectra present a decreasing peak at 515 nm and two growing bands around 600 nm and 396 nm. Considering the system Fe^{II} L_3 / $Fe^{III}L_3$ as the only absorbing compounds responsible for this spectral evolution is insufficient because it does not take into account the increasing concentration of the products formed in the discharge in humid air. The main products are actually nitrate ions, hydrogen peroxide and transient nitrite ions. Hydrogen peroxide and the derived species absorb UV light at wavelengths shorter than 320 nm and thus are not directly concerned. The same conclusion holds for nitrate ions which absorb between 260 and 340 nm with a peak

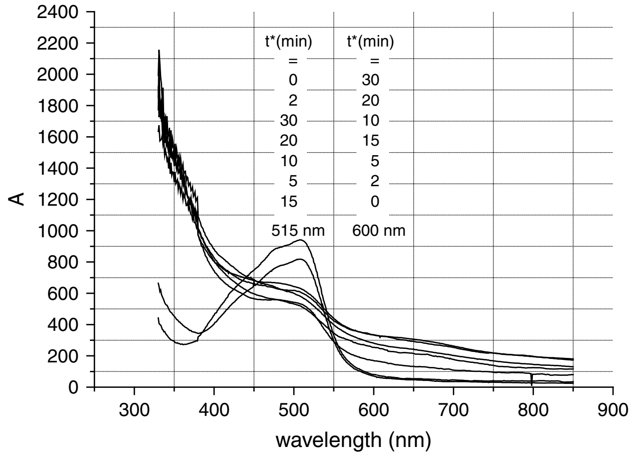

Fig. 3. Evolution of the absorbance spectra (1000 A) of the target solution directly exposed to the discharge for various times *t**. Absorption peaks are evidenced for ferroïn complex recorded immediately after switching on the discharge. Absorption peaks at 515 nm for ferroïn and 600 for ferriïn.

at 304 nm, at the same wavelength as peroxynitrous acid. Oppositely, when nitrite ions are present (as well as nitrous acid) in acid medium, i.e., at a pH where disproportionation into °NO and NO_3^- does not take place, they largely absorb in the 320–400 nm band and present 6 absorption peaks around 360 nm, so that the band feet may interfere with that of the iron complex.

The ligand field of the three molecules of Phenanthroline is strong and the new complex has a weak spin, $S = 0$; with strong oxidizing agents produced by plasma discharges, the iron(III) complex ion is formed, which has a pale blue color. This removal of one electron gives a trivalent iron(III) complex, with five electrons in orbital *d*, *d*5; $S = 1/2$; such a structural modification of the orbitals (metal/ligand) justifies the absence of a peak at 600 nm. However we observe an increase of the band. Reading the band intensity at 396 nm gives the total iron complexed because the absorbances are additive. The light reduction in the band with 396 nm would correspond to the degradation of the ligand by the oxidizing species of plasma.

The decrease in the peak intensity of ferroïn at 515 nm clearly suggests that the complex disappears. This feature may be related either to the dissociation or oxidation of the complex.

- In the first case, the plasma species should attack at the ligand and let the concentration of metal ion increase. Since the plasma treatment induces the formation of hydrogen peroxide, then the occurrence of Fenton's reaction should take place and significantly increase the kinetic rate, which disagrees with the experimental results.

In the event of only one or two ligands are removed as a consequence of acidic effect, lower complexes $Fe^{II}L$ and $Fe^{II}L_2$ would form with increasing concentration. Their spectra are probably different (Table 2) from that of the 1:3 complex with absorption peaks at shorter wavelengths. The occurrrence of an isosbestic point in the spectra file should confirm this assumption, which is not verified experimentally.

- In the second case, the complex $Fe^{II}L_3$ is oxidized into $Fe^{III}L_3$ according to the equilibrium:

$$Fe^{II}L_3 + Ox = Fe^{III}L_3 + Red \tag{17}$$

where the Ox species are generated by the discharge. The formation of $Fe^{III}L_3$ is directly related with the disappearance of the reduced complex and showed by the occurrence of an isosbestic spectral network. This feature is actually observed at 542 nm.

This conclusion is not yet fully satisfactory because the model does not account for the plateau of absorbance observed for $t^* > 10$ min. (Fig. 4) and thus requires more careful consideration. Another serious argument is provided by the chemical properties of peroxynitrous acid which is known for forming nitrate derivatives, as evidenced by its action on thyrosine. In the present case, ONOOH may react with the ligand and form 5-nitro-1.10 phenanthroline (L′). L′ is a base, as is L, with a pK_a around 4 according to authors [11]. The $Fe^{II}L'_3$ complex absorbs at 510 nm ($\varepsilon = 11500$). The standard oxidation potential of $Fe^{II}L'_3$ is reported [11] at 1.30 V/SHE, i.e., at a slightly higher value than for the $Fe^{III}L_3/Fe^{II}L_3$ system. Additionally,

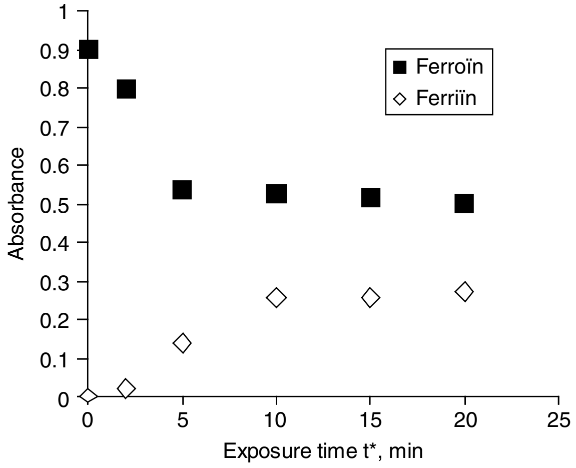

Fig. 4. Effect of the direct exposure time *t** on the absorbance of ferroïn (512 nm) and ferriïn (604 nm) complex solutions.

the oxidized form $Fe^{III}L'_3$ is yellow, and its formation in limited quantities could balance the limited absorbance of ferriïn and its weak absorption coefficient: thus the absorbance of the solution at 604 nm due to a non negligible band foot, should remain quasi constant (Fig. 4).

Briefly, a first sight of the reaction mechanism may be proposed on the basis of the above arguments and involves simultaneous reactions of the Fe-L and Fe-L′ complexes:

$$\begin{array}{l} Fe^{II}L_3 + Ox \;=\; Fe^{III}L_3 + Red \\ \downarrow (ONOOH) \\ Fe^{II}L'_3 + Ox \;=\; Fe^{III}L'_3 + Red \end{array} \qquad (18)$$

This elementary model accounts for the observed phenomena but remains preliminary to a more developed kinetic study in progress. It however confirms that oxidation phenomena take place and that electron exchange with the metal center occurs before the degradation of the ligand.

The essence of the oxidation process is allotted to the primary entities °OH created in the discharge [2,3,5,7,13,14] and reacting at the liquid plasma/target interface. However the formation of secondary species soluble in water with strong oxidizing capacity such as H_2O_2 or ONO_2H occurs in the gas phase and at the interface, so that the compounds drift in the solution where reactions with the solutes may develop. The logarithm transform of the absorbance at the absorption peak of $Fe^{II}L_3$ allows to estimate the constant of a pseudo-1st order kinetic rate around $4*10^{-2}$ min^{-1} with a limited accuracy .

We have now to check whether the observed evolution of the target is limited or not to exposure to the discharge.

3.2. *Effect of humid air flow on the oxidation of ferroïn complex*

A better appreciation of the oxidizing capacity of the species created by the discharge resulted from checking the influence of the air flow on the absorbance peaks of the $Fe^{II}L_3$ and $Fe^{III}L_3$ complexes exposed to the discharge for t^* = 15 min. Fig. 5 shows variations almost similar to those illustrated by Fig. 4. This leads to justify the fact that an increase in air flow leads to an increased quantity of the formed reactive species. The plateau observed for flows between 600 l/h and 800 l/h might be due to saturation of the liquid surface.

3.3. *Effect of post-discharge time on the oxidation of ferroïn complex*

The second aim of this work is devoted to checking whether oxidation reactions develop or not in the target out of the reactor, i.e., in temporal post-discharge conditions (TPDR) [2]. Taking into account the short lifetime of the °OH radical and the formation of the matching dimer, hydrogen peroxide, the system H_2O_2/H_2O becomes the principal oxidizing agent after the discharge is switched-off, if one excepts the oxidizing power of ONO_2H which is well known by Biologists (Table 1). Recording the evolution of the treated solution absorbance at fixed wavelengths highlights a significant decrease of the ferroïn concentration (Fig. 6a) and a matching increase of ferriïn (Fig. 6b) in post-discharge conditions .

Previously detected TPDR examples [2] were found to develop according to pseudo-1st order kinetic laws, and it was suggested that the post–discharge process

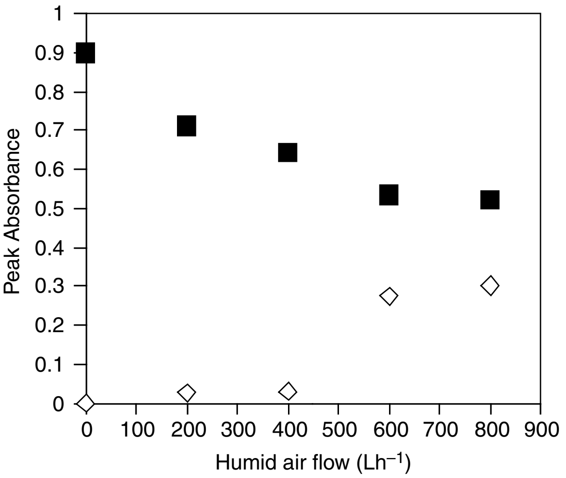

Fig. 5. Effect of humid air flow (lh^{-1}) on the absorbance peaks of the iron complexes (ferroïn: filled squares; ferriïn: empty diamonds) for t^* = 15 min.

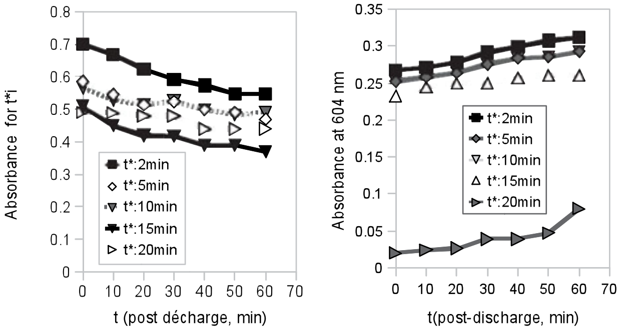

Fig. 6. Evidence of post discharge phenomena on the absorbance of the complexes; A, Left: ferroïn (λ = 512 nm) and B, Right: ferriïn (λ = 604 nm) depending on the exposure time t^*.

was diffusion controlled and involved solute species derived from the impinging secondary species. In the present case, the main reaction

$$Fe^{II}L_3 + ½\, H_2O_2 + H^+ \rightarrow Fe^{III}L_3 + H_2O$$

is governed by the pseudo 1st order kinetic laws:

$$-\frac{dC(Fe^{II}L_3)}{dt} = \frac{dC(Fe^{III}L_3)}{dt} = kC(Fe^{II}L_3) \qquad (19)$$

assuming that the peroxide and proton concentrations remain quasi constant. In terms of absorbances A, which are directly proportional to the concentrations, Eq. (19) becomes:

$$\mathrm{Ln}\,\frac{A_t - A_\infty}{A_0 - A_\infty} = -kt \qquad \text{or} \qquad \mathrm{Ln}(A_t - A_\infty) = -kt + Cst \; (20)$$

where $A_{0,}$ A_∞ and A_t refer to the absorbances at the absorption peak of disappearing $Fe^{II}L_3$ respectively at $t = 0$, at infinite time and at the post-discharge time t. The constant is determined from the limit ($t = 0$). The kinetic constant k involves the concentration of H_2O_2 which directly depends on the exposure time t^* to the discharge.

Considering now the formation of $Fe^{III}L_3$, with absorption measurements at the absorption peak of the oxidized form. $C(Fe^{III}L_3)$ and $C(Fe^{II}L_3)$ are respectively proportional to $(A'_t–A'_0)$ and $(A'_\infty–A'_0)$ – $(A'_t–A'_0)$ = $(A'_\infty–A'_t)$. Thus Eq. (19) becomes (21):

$$d(A_0' - A_t') = -k'(A_\infty' - A_t')dt \qquad (21)$$

and the integer form is, with the limit conditions:

$$\mathrm{Ln}\,\frac{A_\infty' - A_t'}{A_\infty' - A_0'} = -k't \qquad (22)$$

Plotting the logarithm transform of the absorbance values according to Eqs. (20) and (22), allows to confirm the basic assumption of a pseudo first order kinetic mechanism and estimate the apparent kinetic constants for the disappearance of $Fe^{II}L_3$ (Fig. 7).

The evolution of the solution in post-discharge conditions is largely affected by the exposure time t^* to the plasma. This phenomenon is the more important since the exposure time is longer which agrees with the assumed formation of H_2O_2 and the occurrence of this compound in TPDR. Table 3 allows us to check that the kinetic constants k and k' are very similar, which shows that possible side reactions such as the formation of 5-nitro-1,10-phenanthroline do not considerably alter the kinetics. The constants depend on t^* (Fig. 8) and decrease as t^* increases as observed in other cases.

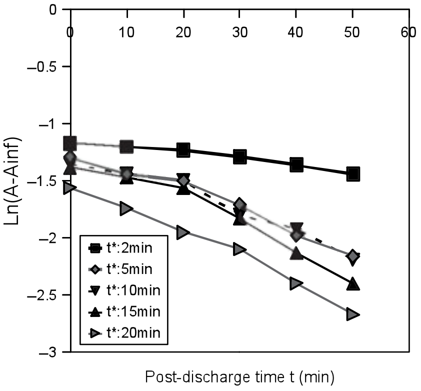

Fig. 7. Kinetic behaviour of ferroïn solutions in post-discharge conditions. The plots Ln[A–A_{inf}] are linear functions of the post-discharge time. A refers to the Absorbance at 512 nm which tends to the value A_{inf} for infinite time.

Table 3
Comparison of the pseudo 1st order kinetic constants for the disappearance k of ferroïn and the formation k' of ferriïn under post-discharge conditions for various exposure times t^*

t^* (min)	2	5	10	15	20
1000*k	4.6	3.6	4.2	2.1	1.6
1000*k'	4.4	3.2	3.2	2.1	2.1

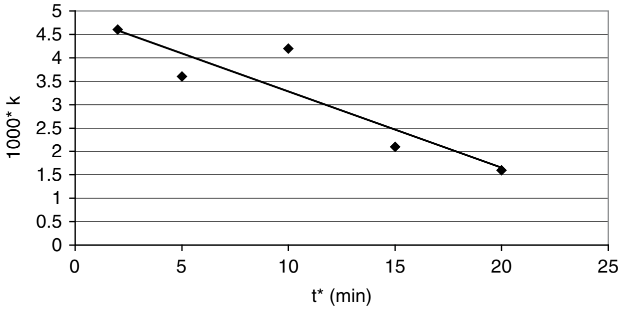

Fig. 8. Influence of the exposure time t^* to the discharge on the post-discharge disappearance constant k of $Fe^{II}L_3$.

This feature may be related to the consumption of H_2O_2 and the resulting decreasing concentration when the discharge is switched off.

4. Conclusion

The major aim of this work is to evaluate the oxidizing properties of gliding arc discharges. The first important result brought by this study is that oxidation of iron complexes readily takes place before its destruction: this feature is illustrated by oxidation of ferrocene. Exposing solutions of 1,10-Phenanthroline ferrous complex to the gliding arc confirms the oxidizing power of humid air discharges. Measurements performed just after switching-off the discharge show that the absorbance of the treated solution decreases with the processing time. This chemical effect is attributed to the presence of the oxidizing couples HO°/H_2O and the derived dimer H_2O_2 / H_2O which react to the surface of the target solution on direct exposure of the target.

Additionally, the oxidation reactions also develop in post-discharge conditions i.e., when the discharge is switched off, on the other hand, the oxidizing capacity would be mainly attributed to the couple H_2O_2/H_2O since the lifetime of HO° radical is very short in aqueous solution. Pseudo-first order kinetics associated with diffusion phenomena thus take place and extend the action of the plasma treatment without extra energy cost, so that this temporal phenomenon of post-discharge is an important parameter in wastewater treatment by gliding arc plasma.

Acknowledgement

This work was supported by International Foundation of Science (Grant W4219-1). The authors highly appreciated this help for improving equipment and facilities.

References

[1] A. Czernichowski, Gliding arc Application to engineering and environment control- Pure Appl. Chem., 66 (1994) 1301–1310.

[2] J.-L. Brisset, D. Moussa, D. Doubla, E. Hnatiuc, B. Hnatiuc, G. Kamgang Youbi, J.-M. Herry, M. Naïtali and M.-N. Bellon-Fontaine, Chemical reactivity of discharges and temporal post discharges in plasma treatment of aqueous media: example of gliding arc discharge treated solutions, A Review - Ind. Eng. Chem. Res., 47 (2008) 5761–5781.

[3] B. Benstaali, B. Cheron, A. Addou and J.-L. Brisset, Spectral investigation of a gliding arc in humid air: a key for chemical applications, Proc. IUPAC Congress ISPC–14 (Int. Symp. Plasma Chem.; Prague, Czech Rep. 1999) H. Hrabowski, M. Konrad and V. Kopecky Eds.; Vol.2. pp. 939–944.

[4] S. Brethe-Dupouey, R. Peyrous and B. Held, Removal of H_2S in air by using gliding arc discharges, Europ Phys J. Appl. Phys., 11 (2000) 43–58.

[5] A. Doubla, S. Laminsi, S. Nzali, E. Njoyim, J. Kamsu-Kom and J.-L. Brisset - Organic pollutant abatement and biodecontamination of brewery effluents by a non-thermal plasma at atmospheric pressure, Chemosphere, 68 (2007) 332–337.

[6] D. Moussa, J.-L. Brisset, E. Hnatiuc and G. Decobert, Plasmachemical destruction of Trilaurylamine from nuclear reprocessing laboratories, Ind. Eng. Chem. Res., 45 (2006) 30–33.

[7] D. Moussa and J.-L. Brisset, Disposal of spent tributylphosphate by gliding arc plasma, J. Hazard. Mater., 102 (2003) 189–200.

[8] B. Benstaali, D. Moussa, A. Addou and J.-L. Brisset, Plasma treatment of aqueous solutes: some chemical properties of gliding arc in humid air, Europ Phys J. Appl. Phys., 4 (1998) 171–179.

[9] F. Depenyou Jr., A. Doubla, S. Laminsi, D. Moussa, J.-L. Brisset and J.-M. Le Breton, Corrosion resistance of AISI 1810 Carbon steel in NaCl 0.5 M solutions by plasmachemical formation of a barrier layer, Corros. Sci., 20 (2008) 1422–1432.

[10] E. Bishop, “Indicators”, Pergamon Press, Oxford (1972).

[11] A.A. Schilt, “Analytical applications of 1,10 phenanthroline and related compounds”, Pergamon Press, Oxford (1969).

[12] A. Czernichowski, Gliding discharge reactor for H_2S valorisation or destruction - in Non-thermal plasma techniques for pollution control (B. Penetrante & S. Schultheis Eds.); Springer-Verlag, Berlin (1992) NATO ASI Series G34 Part B pp. 371–385.

[13] R. Burlica, M. Kirkpatrick, W. Finney, R. Clark and B. Locke, Organic dye removal from aqueous solution by glid arc discharge, J. Electrostat., 62 (2004) 309–321.

[14] A. Doubla, L. Bouba, M. Fotso and J.-L. Brisset, Plasmachemical decolourization of bromothymol blue by gliding arc discharge, Dyes. Pigm., 77 (2007) 118–124.